Journal of Experimental and Applied Physics
Journal Homepage: jeap.ppj.unp.ac.id
Vol. 4, No. 1, March 2026.
ISSN (Print): 2988-0378 ISSN (Online): 2987-9256

Portable Impedance Spectrometer for Characterizing the Electrical Properties of Dielectric Materials using A Goertzel Filter

M Zikri Arifin[1,*], Mairizwan[1], Asrizal[1], Mona Berlian Sari[1]
[1] Department of Physics, Universitas Negeri Padang, Padang 25131, Indonesia

Article History
Received : January, 26th 2026
Revised : February, 03rd 2026
Accepted : February, 04th 2026
Published : March, 31st 2026

DOI:
https://doi.org/10.24036/jeap.v4i1.166

Corresponding Author
*Author Name: M Zikri Arifin
Email: mzikri.arifin4@gmail.com

Abstract: Dielectric materials have the ability to store large amounts of electrical energy, which is useful in electronics, such as in the manufacture of capacitors. However, the equipment available for characterization is usually quite complex and expensive. Therefore, this study aims to develop a highly portable embedded impedance spectrometer for characterizing the electrical properties of dielectric materials, namely complex permittivity and dissipation factor, and then demonstrate the effect of increasing the test frequency on the measurement results. The system consists of an STM32F407 microcontroller, an AD9850 DDS as an AC signal generator, and a Goertzel filter algorithm for signal processing. The results of testing the system with paper dielectric samples showed an accuracy of 89.37% for real impedance and 93.22% for imaginary impedance. The results of the paper dielectric sample characterization show an increase in the real value of complex permittivity in the 1kHz-10kHz frequency range, while the imaginary value shows an increase from 1kHz-5kHz and then stabilizes up to 10kHz. The increase in frequency also shows an increase in the dissipation factor (dielectric loss) at each increase in frequency. The results of the study show that the impedance spectrometer system provides an innovative solution in the field of material characterization.

Keywords: Dissipation Factor, Complex Permittivity, Goertzel Filter, Impedance Spectrometer, Imaginary Impedance, Real Impedance

1. Introduction

Research in the field of materials continues to develop rapidly [1]. Researchers continue to conduct studies to obtain higher quality materials that can be applied in various fields. One of the materials currently being developed is dielectric material due to its enormous benefits. Dielectric

How to cite:
Z. Arifin, Mairizwan, Asrizal, M.B. Sari, 2026, Portable Impedance Spectrometer for Characterizing the Electrical Properties of Dielectric Materials using A Goertzel Filter, *Journal of Experimental and Applied Physics,* Vol. 4, No. 1, page 1-14. https://doi.org/10.24036/jeap.v4i1.166

material is a material that has the ability to store electrical energy [2]. Based on this capability, dielectric materials have been widely developed in various fields of research. In electronics, dielectric materials are typically used in the manufacture of electronic components, such as dielectric materials for capacitors[3], material for making a single-element square microstrip antenna [4], and cable coating materials[5]. The application of dielectric materials in the field of electronics is inseparable from the application of their electrical properties.

Characterization of the electrical properties of materials refers to the measurement and analysis of the electrical properties of those materials. Electrical properties are the characteristics of a material when an electric charge is present [6]. In dielectric materials, these electrical properties greatly affect their quality, such as dielectric constant and dissipation factor. Dielectric constant or relative permittivity reflects a material's response to an external electric field and has become one of the most important topics in physics [7]. Meanwhile, the dissipation factor (tan delta or loss tangent) is a parameter that measures the ratio of stored energy to lost energy in a material [8]. The dissipation factor can be measured at a single frequency or over a wide frequency range using spectroscopy methods [9].

Spectroscopy methods that can be used to measure the electrical properties of materials such as dielectric constants and dissipation factors are impedance spectroscopy. Impedance spectroscopy is a measurement technique used in various applications and fields, including material characterization and testing. The measurement procedure with impedance spectroscopy involves applying an excitation signal such as current and voltage, and then measuring the voltage and current response to measure impedance [10]. Then, from the impedance, the dielectric constant and dissipation factor of a material can be obtained.

In several previous studies, the dielectric properties of Calcium Copper Titanate material were measured using computerized impedance spectroscopy with an embedded system using a microcontroller [2]. Although computerized, the system developed in this research has not yet utilized a portable signal generator component, and the system automation still requires significant human involvement in its operation. Research conducted in 2020 [11], shows that impedance spectroscopy can be applied to smaller, energy-efficient, and inexpensive devices using an STM32F407 microcontroller, AD9850 DDS, instrumentation amplifier, and Discrete Fourier Transform (DFT) algorithm for signal analysis. However, it still uses a fairly complex algorithm, which consumes a significant amount of memory, especially in embedded systems. A study in 2022 [12], comparing several AC signal processing methods such as Fast Fourier Transform (FFT), Goertzel Filter, Discrete-Time Fourier Transform (DTFT), and Sine Fitting, based on speed, memory requirements, and accuracy, found that the most efficient method overall is the Goertzel Filter, particularly for systems with limited memory.

Thus, based on the limitations of the systems in those studies, this research aims to design an impedance spectrometer to measure the electrical properties of dielectric materials in the form of complex permittivity and dissipation factor and determine their relationship with the measurement frequency. The system is designed to have a high level of portability using the STM32F407 microcontroller, AD9850 DDS for AC signal generation, and a simpler signal processing system than DFT, namely the Goertzel algorithm.

2. Materials and Method

The type of research conducted is engineering research. Engineering research involves the process of designing, developing, testing, and evaluating until it becomes a product or prototype. [13]. Engineering research can be conducted using various methods depending on the product design and research objectives. The result of this research is a portable impedance spectrometer for measuring complex permittivity and dissipation factor.

This research was conducted by collecting information related to the research topic. The impedance spectroscopy system was created using electronic components consisting of a signal generator, microcontroller, and signal processing algorithm. The system was first arranged geometrically in a block diagram as shown in Figure 1.

The impedance spectrometer system consists of three main processes, namely the process of exciting the AC signal to the sample, the process of amplifying the signal using an instrumentation amplifier, and then the process of signal processing in a microcontroller. The components used in these three processes consist of an AD9850 signal generator, the material being tested which is placed between two conductor plates driven by a servo, an instrumentation amplifier with a circuit as shown in Figure 2, and an STM32F407VET6 microcontroller as the analysis and control component.

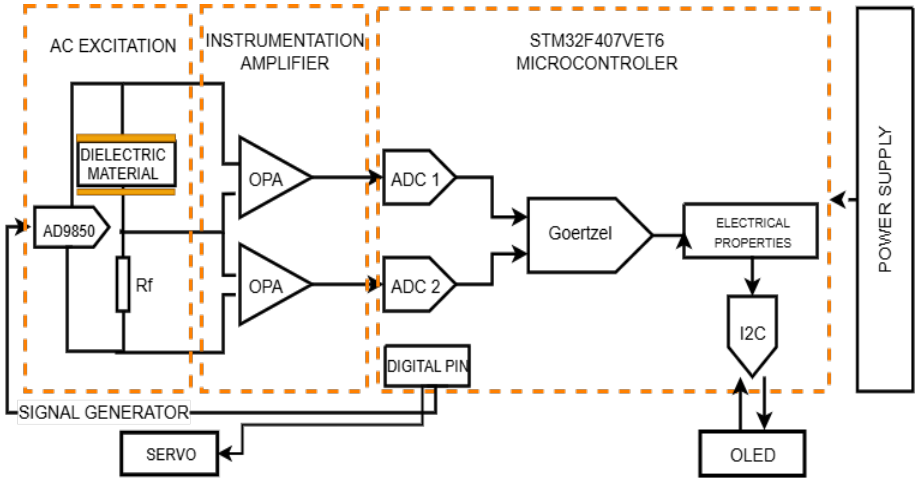

Figure 1. System block diagram

The AD9850 plays an important role as an AC signal source in the 1kHz-10kHz frequency range. The instrumentation amplifier amplifies the received voltage response and transmits each to ADC1 and ADC2 on the microcontroller. The voltage response received by ADC2 from the voltage on the reference resistor is converted into current, while the voltage from the test material received by ADC2 is not converted. This voltage and current data is arranged in an array to be converted into the frequency domain by the Goertzel Filter signal analyzer, which produces the phase and magnitude of the voltage and current signals. Calculations are then performed to obtain the electrical properties of the test material, such as impedance, permittivity, and dissipation factor (dielectric loss). The calculation results are displayed on an OLED sent via the microcontroller's I2C.

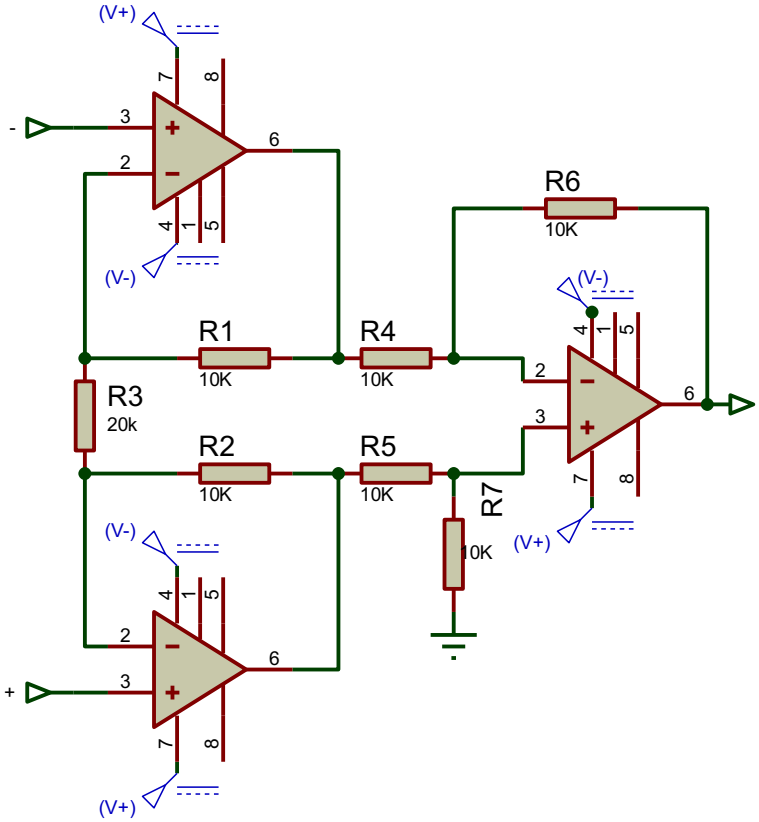

Figure 2. Schematic of the instrumentation amplifier

The instrumentation amplifier circuit consists of two non-inverting amplifiers and one differential amplifier, so that the total gain is the product of the non-inverting gain and the differential gain.

The total reinforcement is calculated using the equation[14]:

$$P = \left(1 + \frac{2R_1}{R_3}\right) \times \frac{R_7}{R_5} \quad (1)$$

With $R_1 = R_2, R_4 = R_5, dan\ R_6 = R_7$, so that the output voltage will be obtained with the equation[14]:

$$v_{out} = P \times v_{in} \quad (2)$$

The design of the impedance spectrometer system consists of hardware mechanical design and software design. The hardware design is a mechanical design combined with an electronic circuit consisting of several supporting components in the system, as shown in Figure 3. The software design is a system flowchart, as shown in Figure 4.

2.1. System Hardware Design

The hardware design consists of a mechanical design combined with an electronic circuit consisting of several supporting components in the system, as shown in Figure 3.

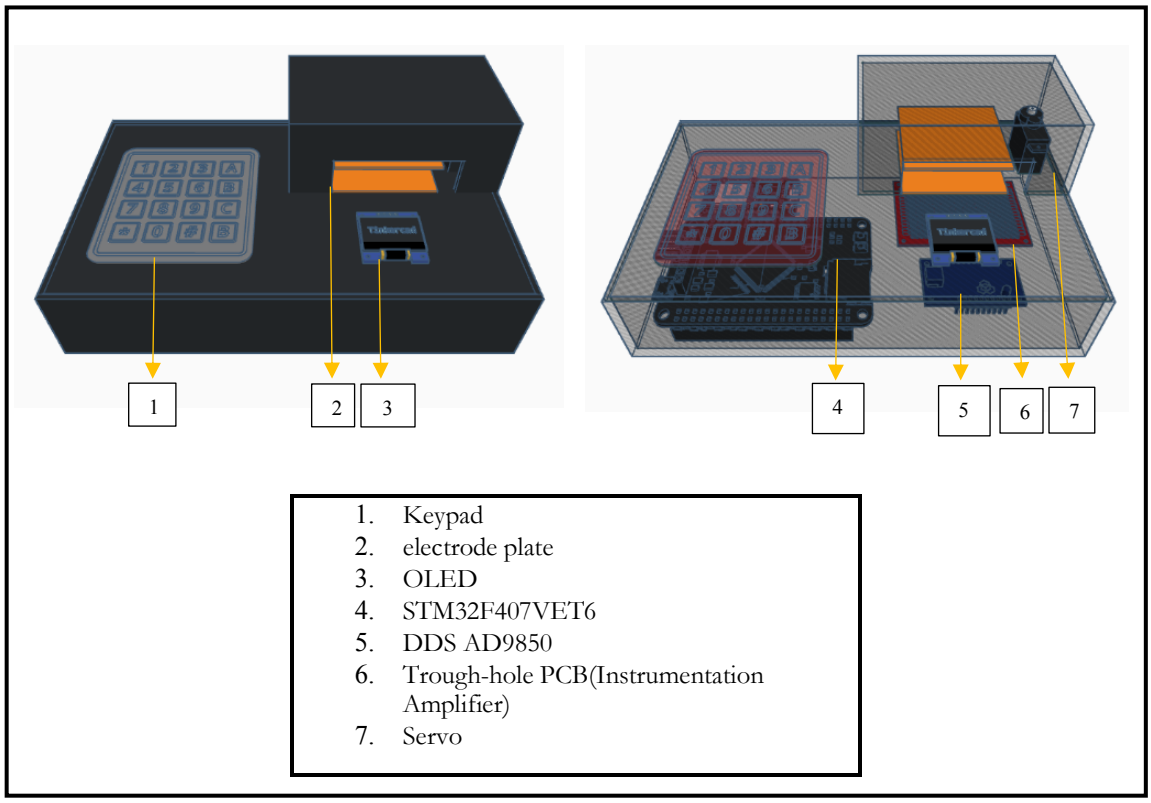

Figure 3. Hardware Design

2.2. System Software Design

2.2.1. Flowchart

The system flowchart covers all measurement processes from initial sample initialization, signal processing, to obtaining measurement results, as shown in Figure 4. When the active measurement system starts from the frequency input that will be excited by the DDS (Direct Digital Synthesis) AD9850 and then received by the ADC pin on the microcontroller. The ADC data is then converted to voltage and current, which is then stored in an array. Then the Goertzel algorithm is applied to the voltage and current data array that has been converted from the ADC value to obtain the magnitude and phase. This data is then used to obtain the impedance values and electrical properties of the material.

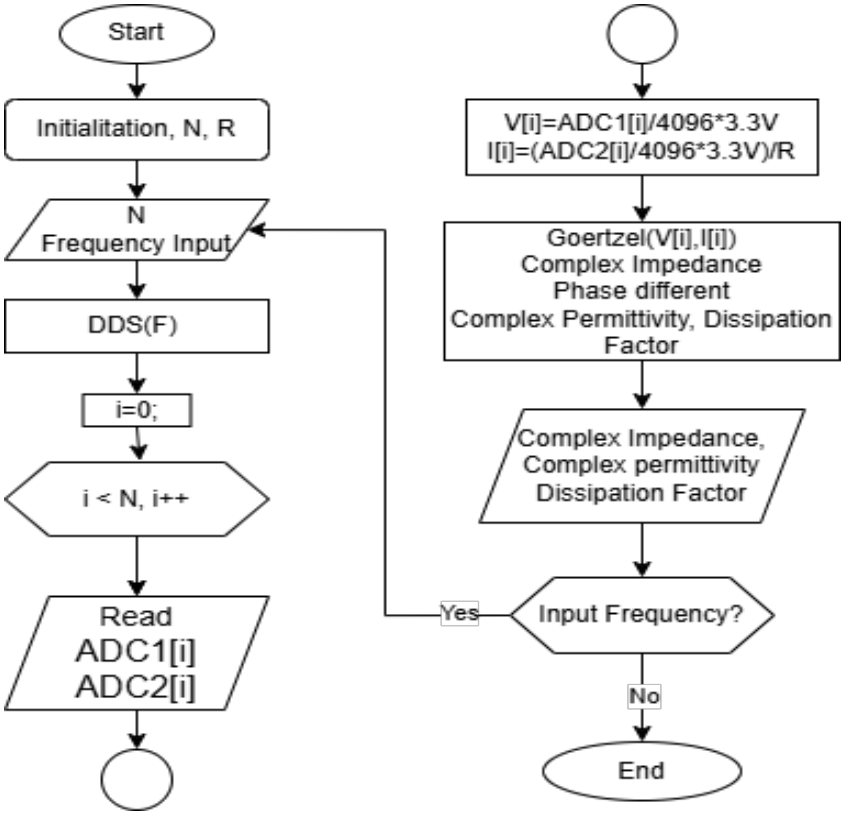

Figure 4. Impedance spectrometer system flowchart

2.2.2. Implementation with Goertzel Filter

In impedance spectroscopy, to obtain impedance, the amplitude and phase values of the signal are required [10]. To determine the amplitude and phase using Fourier transform-based methods such as Discrete Fourier Transform (DFT)[12]. DFT calculations can be performed using the Goertzel Filter algorithm by placing the DFT on the filter.

The Goertzel algorithm (Goertzel filter) was introduced in 1950 by Gerald Goertzel to calculate one bin from the DFT, namely bin k defined in [15]:

$$X[k] = \sum_{n=0}^{N-1} x[n] e^{-j2\pi k \frac{n}{N}}, \quad k = 0, \ldots\ldots, N-1 \tag{3}$$

which can be implemented as a second-order Infinite Impulse Response (IIR) filter that is a transfer function in the z domain defined in [15]

$$h_k[z] = \frac{1 - e^{j\frac{2\pi k}{N}} z^{-1}}{1 - 2\cos\left(\frac{2\pi k}{N}\right) z^{-1} + z^{-2}} \tag{4}$$

From this, we can derive a second-order difference equation, which is the final result of the recursive form of the goertzel algorithm, and the output formula DFT k^{th} [15]

$$s[n] = x[n] + 2\cos\left(\frac{2\pi k}{N}\right) s[n-1] - s[n-2] \tag{5}$$

$$y_k[n] = s[n] - e^{-j\frac{2\pi k}{N}} s[n-1] \tag{6}$$

From the second-order difference equation, an algorithm can be created as shown in Table 1, where the real and imaginary components of the DFT are extracted when the number of iterations reaches the number of samples N, which are applied to the current and voltage signals, respectively. For spectroscopy systems that measure a single target frequency, the frequency bin index is modeled with $k = \frac{Nf_{target}}{f_s}$ then the algorithm becomes [12].

Goertzel Filter Algorithm

Input: f: target frequency, fs: sampling frequency
Output: Y: signal magnitude output in the form of complex values

a ← $cos(\frac{2\pi f}{fs})$;

b← $sin(\frac{2\pi f}{fs})$;

s[n] ← $x[n] + 2a.s[n-1] - s[n-2]$;

Y ← $complex(a.s[n-1] - s[n], b.s[n-1])$;

$|Y| \leftarrow 2\frac{\sqrt{Y_{real}{}^2 + Y_{imag}{}^2}}{N}, \qquad \varphi_y = atan2(Y_{imag}, Y_{real}) + \frac{\pi}{2}$

$x[n]$ is the input signal, $Y_{real} = a.s[n-1] - s[n]$ real part from magnitude and $Y_{imag} = b.s[n-1]$) imaginary part.

Using the same algorithm, the amplitude and phase for the current and voltage signals are modeled with [12]:

$$|V| = 2\frac{\sqrt{V_{real}{}^2 + V_{imag}{}^2}}{N}, \qquad \varphi_v = atan2(V_{imag}, V_{real}) + \frac{\pi}{2} \tag{7}$$

$$|I| = 2\frac{\sqrt{I_{real}{}^2 + I_{imag}{}^2}}{N}, \qquad \varphi_I = atan2(I_{imag}, I_{real}) + \frac{\pi}{2} \tag{8}$$

$$\Delta\varphi = \varphi_v - \varphi_I \tag{9}$$

Signal impedance is modeled with [16] :

$$|Z| = \frac{|V|}{|I|}, \quad Z_{real} = |Z|\cos(\Delta\varphi), \quad Z_{imag} = |Z|\sin(\Delta\varphi) \tag{10}$$

2.2.3. Calculation of Complex Permittivity and Dissipation Factor

Complex permittivity consists of a real part (ε_{real}) and the imaginary part(ε_{imag}), provided by [17]:

$$\varepsilon_{real} = \frac{-dZ_{imag}}{\omega\varepsilon_0 A({Z_{real}}^2 + {Z_{imag}}^2)}, \quad \varepsilon_{imag} = \frac{dZ_{real}}{\omega\varepsilon_0 A({Z_{real}}^2 + {Z_{imag}}^2)} \tag{11}$$

Dielectric loss or dissipation factor or loss tangent ($\tan\delta$) is the ratio between stored energy and lost energy [17]:

$$tan\delta = D = \frac{\varepsilon_{imag}}{\varepsilon_{real}} \tag{12}$$

3. Results and Discussion

3.1. System Hardware

The mechanics of this impedance spectrometer system are constructed using acrylic with a thickness of 3 mm. The manufacturing process begins with designing each component in Tinkercad, followed by cutting and assembling them as shown in the figure 5. The mechanical system in Figure 5 is constructed in a compact size to enhance its portability, with dimensions of 20 cm x 12 cm x 4 cm. The mechanism is designed to provide sufficient space for all necessary components, such as the STM32F407 microcontroller, DDS AD9850, servo, OLED, keypad, and other supporting components. On the top, there is a sample placement area consisting of parallel electrode plates, which are adjusted by a servo to increase the automation of the system.

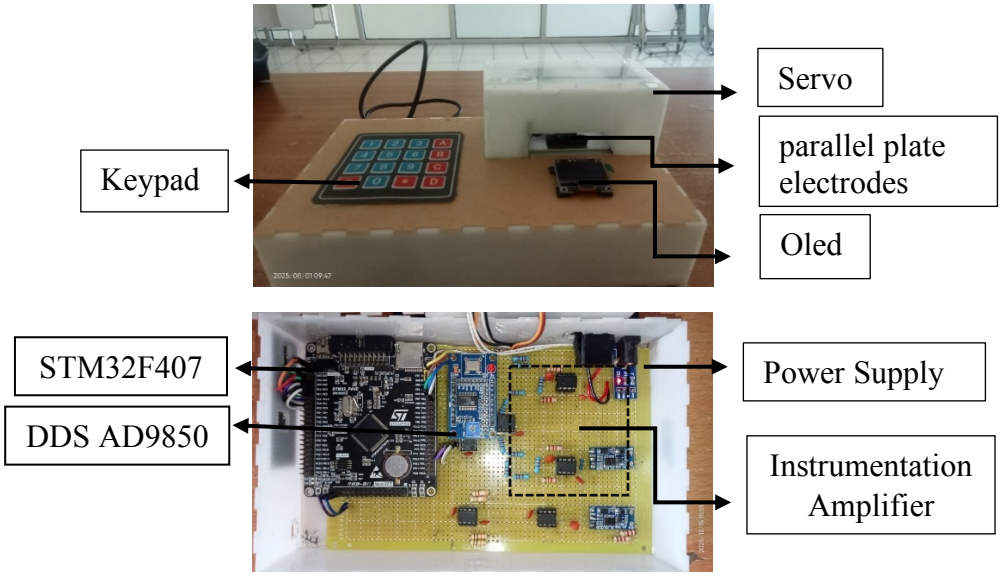

Figure 5. System hardware

The components forming the system are assembled in an electronic circuit using a PCB with dimensions of 18 cm x 12 cm. The entire system is powered by an adapter with a voltage of 5V. The instrumentation amplifier circuit is shown in Figure 5, consisting of three OPA2134 ICs powered by ±12 V from a step-up module (the blue one). The two other ICs in Figure 20 are used as buffers and summing amplifiers to provide a DC offset to the signal so that the entire signal range can be read by the microcontroller.

3.2. *System Testing*

The test was conducted by comparing the results of complex impedance measurements using an impedance spectrometer and an LCR meter in the frequency range of 1kHz-10kHz. The test was necessary to determine the percentage of error and accuracy of the impedance spectrometer that had been made using paper dielectric samples placed on the test field between two parallel plate electrodes.

Real impedance measurements using an impedance spectrometer provide two types of data, namely real impedance and imaginary impedance. Impedance values on an LCR meter are measured using series mode, where the measurement results display the resistance (R) and capacitance (C) values with a total impedance of Z=R + $\frac{1}{j\omega C}$, where Rs indicates real impedance and $\frac{1}{j\omega C}$ indicates imaginary impedance. The error and accuracy percentage tables are as shown in Table 1 for real impedance values and Table 2 for imaginary impedance values.

Table 1. Real impedance measurement data

Frequency (kHz)	Impedance Spectrometer (kΩ)	LCR Meter (kΩ)	Error(%)	Accuracy(%)
1	75,042	80,47	6,74	93,26
2	45,018	46,95	4.11	95.89
3	35,374	35,12	0,72	99,28
4	29,854	28,77	3,76	96,24
5	25,937	24,08	7,71	92,29
6	22,889	20,83	9,88	90,12
6,7	21,531	19,07	12.9	87,1
7.5	20,041	17,17	16,72	83,28
8.5	18,088	15,16	19,31	80.69
10	16,340	13,13	24.44	75,56
	Average		10,63	89,37

Table 2. Impedance measurement data using an LCR Meter

Frequency (kHz)	Impedance Spectrometer(kΩ)	LCR Meter (kΩ)	Error(%)	Accuracy(%)
1	-378,991	-343,921	10,19	89,81
2	-202,845	-184,300	10,06	89,94
3	-141,174	-131,058	7,71	92,29
4	-110,811	-103,939	6,61	93,39
5	-91,787	-86,776	5,77	94,23
6	-78,598	-74,758	5,13	94,87
6,7	-71,773	-68,642	4,56	95,44
7,5	-65,197	-61,185	6,55	93,45
8,5	-58,072	-54,642	6,27	93,73
10	-50,931	-48,547	4,91	95,09
	Average		6,76	93,22

A comparative graph of impedance measurements using an impedance spectrometer and an LCR meter is shown in Figure 5.

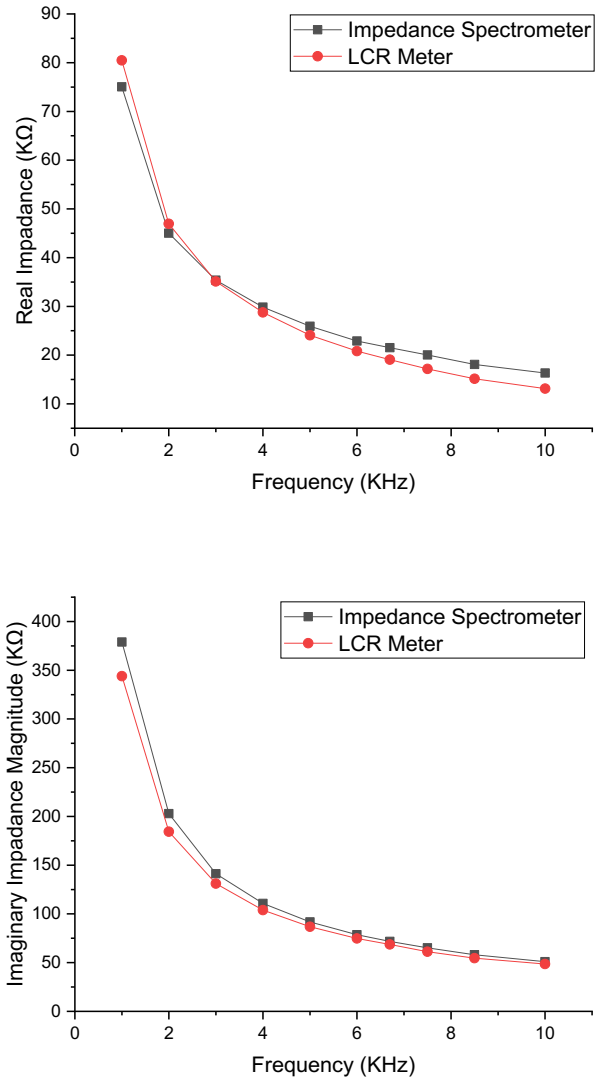

Figure 6. Graph of the relationship between real and imaginary impedance and frequency

From the results of measuring the impedance of each using an impedance spectrometer and LCR meter, which were then compared as shown in Tables 1 and 2, the average percentage error of the instrument in the range of 1 kHz -10 kHz was 10.63% for real impedance values with an accuracy of 89.37% and 6.76% for imaginary impedance with an accuracy of 93.22%. The error increases with each frequency increment, particularly in the measurement of real impedance, in line with the findings of the 2020 study.[18], which indicates a significant increase in parasitic impedance of the internal components compared to the impedance of the tested sample, especially at high frequencies.

3.3. Measurement of Complex Permittivity and Dissipation Factor

Measurement of complex permittivity and dissipation factor using an impedance spectrometer that has been calibrated with a standard device using impedance values. On the impedance spectrometer, measurement of the dielectric properties of materials can be performed using real and imaginary impedance values using equation 11. The dielectric sample measured was paper with a specified surface area of $0{,}25 \times 10^4\ m^2$ and thick $0{,}18 \times 10^3$m performed in the frequency range of 1kHz-10kHz. The measurements aim to determine the relationship between the electrical properties of paper, such as permittivity and dissipation factor, at various frequencies. The measurement data can be seen in Table 3.

Table 3. Measurement data of Complex Permittivity and dissipation factor using an Impedance Spectrometer .

Frequency (kHz)	**Complex Permittivity**		**Dissipation Factor (D)**
	Real Value (ε_{real})	**Imaginary Part (ε_{Imag})**	
1	3,29	0,65	0,198
2	3,04	0,67	0,222
3	2,88	0,72	0,251
4	2,72	0,73	0,269
5	2,61	0,74	0,283
6	2,53	0,74	0,291
6,7	2,48	0,74	0,300
7,5	2,42	0,74	0,307
8,5	2,37	0,74	0,311
10	2,30	0,74	0,321

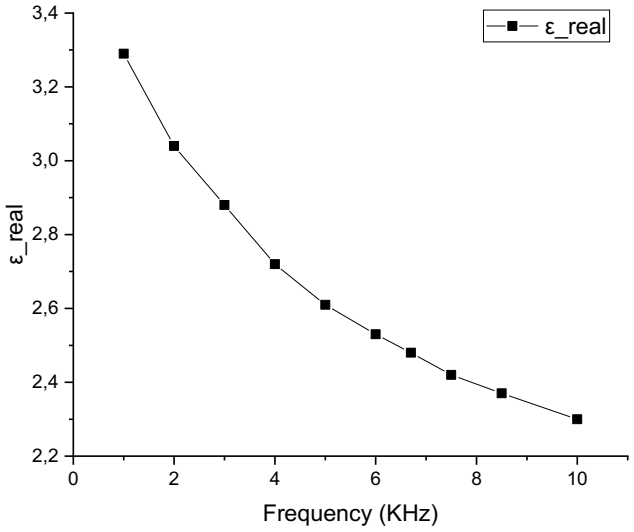

Figure 7a. Graph showing the relationship between real part of permittivity versus frequency

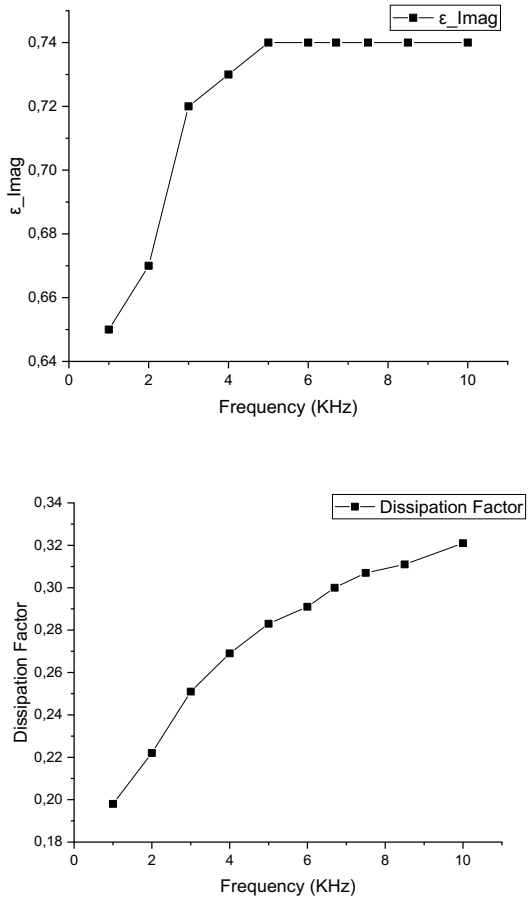

Figure 7b. Graph showing the relationship between imaginary permittivity and dissipation factor versus frequency

Based on the measurement data, the complex permittivity of the sample, namely paper, has a value that is influenced by the measurement frequency. Figure 7 shows the relationship between electrical properties and frequency. The real permittivity of paper dielectric decreases from 3.29 to 2.3 with each increase in frequency in the measurement range of 1kHz-10kHz. Meanwhile, the imaginary permittivity value increases from 0.65 to 0.74 at 1kHz-5kHz and then remains relatively constant at 0.74 up to a frequency of 10kHz. The dissipation factor increases with each increase in measurement frequency from 0.198 to 0.321, indicating that the paper has higher dielectric loss as the frequency increases.

4. Conclusion

This research successfully designed a highly portable impedance spectrometer system with an embedded system and Goertzel filter algorithm for characterizing the electrical properties of dielectric materials. In testing the device, the results showed an average measurement accuracy level

for real impedance of 89.37% and imaginary impedance of 93.22% with an average error rate of 10.63% and 6.76%. The system shows a strong relationship between frequency increase and decrease in real and imaginary impedance values. The system also successfully characterizes the electrical properties of paper dielectric materials, where the measurement results show a close relationship between frequency increase and decrease in dielectric quality, as evidenced by a decrease in permittivity and a significant increase in dissipation factor or dielectric loss at frequencies of 1kHz – 10 kHz. The results of the study show that the impedance spectrometer system provides an innovative solution in the field of material characterization, paving the way for more reliable and efficient research.

Acknowledgments

Thank you to all parties involved, especially the Physics Department of Universitas Negeri Padang, which has provided research support facilities, so that this research can be completed.

References

[1] M. A. Shomad and A. A. Jordianshah, "Pengaruh Penambahan Unsur Magnesium pada Paduan Aluminium dari Bahan Piston Bekas," *Teknoin*, vol. 26, no. 1, pp. 75–82, Jul. 2020, doi: 10.20885/TEKNOIN.VOL26.ISS1.ART8.

[2] W. B. Kurniawan and D. K. Abraha, "Pengukuran Nilai Dielektrik Material Calcium Copper Titanat (Cacu3ti4o12) Menggunakan Spektroskopi Impedansi Terkomputerisasi Measurement Of The Dielectric Constant For Calcium Copper Titanate (Cacu3ti4o12) Materials Using Computerized Impedance Spectroscopy," 2017.

[3] H. P. Teng and F. H. Lu, "Production of Ba(Zr,Ti)O3 coatings on ternary (Ti,Zr)N thin film electrodes by plasma electrolyte oxidation," *Surf. Coat. Technol.*, vol. 385, Mar. 2020, doi: 10.1016/j.surfcoat.2020.125440.

[4] A. Al Shifa, I. Wulani, Y. S. Azzahra, and H. Ludiyati, "Prosiding The 11 th Industrial Research Workshop and National Seminar Bandung," 2020.

[5] S. S. Suresh, S. Mohanty, and S. K. Nayak, "Composition analysis and characterization of waste polyvinyl chloride (PVC) recovered from data cables," *Waste Management*, vol. 60, pp. 100–111, Feb. 2017, doi: 10.1016/j.wasman.2016.08.033.

[6] N. M. Seniari, I. F. Citarsa, and A. Ningsih, "Korelasi Antara Sifat Listrik Dengan Sifat Fisika Dan Sifat Kimia Dari Minyak Transformator," *Dielektrika*, vol. 8, no. 2, pp. 118–125, Aug. 2021, Accessed: Jan. 16, 2025. [Online]. Available: https://dielektrika.unram.ac.id/index.php/dielektrika/article/view/280

[7] N. Yao *et al.*, "An Atomic Insight into the Chemical Origin and Variation of the Dielectric Constant in Liquid Electrolytes," *Angewandte Chemie - International Edition*, vol. 60, no. 39, pp. 21473–21478, Sep. 2021, doi: 10.1002/anie.202107657.

[8] A. Ward, "Dielectric materials for advanced applications," 2016, doi: 10.13140/RG.2.1.3481.5600.

[9] M. Florkowski, M. Kuniewski, and P. Mikrut, "Effect of voltage harmonics on dielectric losses and dissipation factor interpretation in high-voltage insulating materials," *Electric Power Systems Research*, vol. 226, Jan. 2024, doi: 10.1016/j.epsr.2023.109973.

[10] O. Kanoun and A. Y. Kallel, "High-performance efficient embedded systems for impedance spectroscopy: Challenges and potentials," *Electrochim. Acta*, vol. 492, Jul. 2024, doi: 10.1016/j.electacta.2024.144351.

[11] R. Munjal, F. Wendler, and O. Kanoun, "Embedded Wideband Measurement System for Fast Impedance Spectroscopy Using Undersampling," *IEEE Trans. Instrum. Meas.*, vol. 69, no. 6, pp. 3461–3469, Jun. 2020, doi: 10.1109/TIM.2019.2932177.

[12] A. Y. Kallel, Z. Hu, and O. Kanoun, "Comparative Study of AC Signal Analysis Methods for Impedance Spectroscopy Implementation in Embedded Systems," *Applied Sciences (Switzerland)*, vol. 12, no. 2, Jan. 2022, doi: 10.3390/app12020591.

[13] M. Mahmood Ali, "Experimental methods for science and engineering students: an introduction to the analysis and presentation of data, 2nd edition," *Contemp. Phys.*, vol. 61, no. 2, pp. 146–147, Apr. 2020, doi: 10.1080/00107514.2020.1756922.

[14] Z. Abidin, K. Tanno, S. Mago, and H. Tamura, "A new instrumentation amplifier architecture based on differential difference amplifier for biological signal processing," *International Journal of Electrical and Computer Engineering*, vol. 7, no. 2, pp. 759–766, 2017, doi: 10.11591/ijece.v7i2.pp759-766.

[15] L. Ferreyro *et al.*, "An implementation of a channelizer based on a Goertzel Filter Bank for the read-out of cryogenic sensors," *Journal of Instrumentation*, vol. 18, no. 6, Jun. 2023, doi: 10.1088/1748-0221/18/06/P06009.

[16] K. Ariyoshi *et al.*, "Electrochemical Impedance Spectroscopy Part 1: Fundamentals†," *Electrochemistry*, vol. 90, no. 10, 2022, doi: 10.5796/electrochemistry.22-66071.

[17] A. Bendahhou, K. Chourti, R. El Bouayadi, S. El Barkany, and M. Abou-Salama, "Structural, dielectric and impedance spectroscopy analysis of Ba5CaTi1.94Zn0.06Nb8O30ferroelectric ceramic," *RSC Adv.*, vol. 10, no. 47, pp. 28007–28018, Jul. 2020, doi: 10.1039/d0ra05163b.

[18] C. Erinmwingbovo and F. La Mantia, "Estimation and correction of instrument artefacts in dynamic impedance spectra," *Sci. Rep.*, vol. 11, no. 1, Dec. 2021, doi: 10.1038/s41598-020-80468-x.